Journal of The Electrochemical Society, **154** (3) H231-H238 (2007)
0013-4651/2007/154(3)/H231/8/$20.00 © The Electrochemical Society

Comparative Study of Carrier Lifetime Dependence on Dopant Concentration in Silicon and Germanium

E. Gaubas[a] **and J. Vanhellemont**[b]

[a]*Institute of Materials Science and Applied Research, Vilnius University, LT-10223 Vilnius, Lithuania*
[b]*Department of Solid State Sciences, Ghent University, B-9000 Ghent, Belgium*

The increasing use of thin germanium layers on silicon substrates as active layers in advanced electronic devices is the motivation for a comparative study of the dependence of the carrier recombination characteristics on excitation and dopant concentration in both semiconductors. Bulk and surface components of the carrier lifetime are separated by studying samples with different geometries and surface finishing. The bulk carrier lifetime is determined as a function of dopant concentration and in the case of germanium also as a function of the excitation level. The bulk lifetime observations are simulated by combining the lifetime according to Shockley-Read-Hall (SRH) theory with the lifetime resulting from Auger recombination above a doping concentration threshold. It is shown that the bulk carrier lifetime behavior in Si and Ge is very similar. Carrier lifetime changes in Si can be well described by a combined SRH and Auger recombination model, while lifetime variations in Ge fit well the SRH model, taking into account the lifetime dependence on the injection level. It is shown that the lifetime dependence on dopant concentration in germanium can be phenomenologically described by assuming a linear increase of recombination center concentration with dopant concentration. The results also illustrate the importance of surface passivation and of material quality which depends on the fabrication technology, when comparing carrier lifetimes obtained with different equipment and on different samples.
 [DOI: 10.1149/1.2429031]

Manuscript submitted July 6, 2006; revised manuscript received October 26, 2006. Available electronically January 30, 2007.

Carrier lifetime is one of the semiconductor parameters that is very sensitive to the structure and density of lattice defects and to impurities, both native related to the crystal growth process (e.g., oxygen in Czochralski silicon) and contaminants, which can interact with lattice and structure defects, enhancing or reducing the influence of doping and injection levels. The direct measurement of carrier lifetime is therefore a powerful tool to evaluate the quality of semiconductor substrates and layers. The variation of carrier lifetime with doping and excitation level has been widely studied for silicon.[1] The renewed interest for applications of Ge substrates and thin films, with a wide range of resistivities, from high-purity Ge for particle detector applications to highly doped Ge substrates for GaAs epitaxy in solar cells technology, necessitates a better understanding of the carrier recombination properties of Ge. The use of active germanium layers in advanced silicon device structures is the motivation for the comparative study of the dependence of recombination characteristics on excitation and dopant concentration that is presented in this paper.

Two of the main factors limiting the effective carrier lifetime are surface recombination and Auger processes. In silicon, the variation of the recombination lifetime as a function of dopant concentration can be described well by the Shockley-Read-Hall (SRH) recombination model[1] only up to a threshold doping level of the order of 7×10^{15} cm^{-3}.[2] In more heavily doped silicon, the carrier lifetime decreases nearly linearly with increasing doping.[2] This implies a dopant concentration-dependent increase of the concentration of recombination centers. The wide spread of lifetime values reported for similar Si materials using similar measurement techniques, even after correction for surface recombination, is to a large extent related to the recombination regimes involved.

From a methodological point of view, the bulk excitation regime is the most appropriate one to clarify the impact of bulk defects on lifetime, and it is easily implemented for Si by using, e.g., the 1064 nm wavelength light of yttrium aluminum garnet (YAG) lasers. To reveal the impact of surface defects, the main decay mode can be studied by analyzing the decay transients at different excitation wavelengths and levels. This can be performed by simultaneously monitoring the amplitude and the lifetime of the main decay mode.[3] In high-resistivity material, the trapping effect is the main distorting factor to obtain a suitable measurement regime for the recombination lifetime evaluation. The variation in the sensitivity of the photoconductivity probes that are applied in different experiments is also a reason for poorly defined measurement conditions, especially when the excitation level is not carefully controlled. In germanium, due to the limited availability of suitable excitation sources, it is often difficult to establish a suitable bulk excitation regime. Due to that, problems appear when estimating the effective carrier density integration depth, while the relaxation process does not reach the main depth-integrated decay mode.

Another important reason for the wide variation of reported lifetime values is the length of the excitation pulse that is applied. Important decay characteristics, such as the decay shape or deep level filling effects, can indeed be masked by using pulses that are too long. A sharp excitation profile in the range of nonlinear recombination processes is difficult to analyze as it forms of a system of distributed parameters. In such cases even the separation of surface and bulk recombination parameters is not straightforward.

In the present study, carrier lifetime values measured in Si and Ge samples with different dopant concentrations were compared with average lifetime values based on a wide range of data. The expected lifetime variation was simulated using the SRH model combined with Auger recombination above a doping concentration threshold, and the results were compared with the experimental results obtained for different excitation levels and with published experimental data.

Materials studied.— Czochralski (CZ), magnetic field assisted Czochralski (MCZ) and floating zone (FZ) grown silicon samples with resistivities between 0.03 and 7000 Ω cm were investigated. Samples with thicknesses in the range of 0.28 to 5 mm were studied. The surfaces of the thin, high resistivity wafers were passivated by thermal oxidation. The other Si wafers were polished.

CZ and FZ grown Ge wafers from different suppliers were investigated. To examine the role of surface preparation and of surface recombination parameters, samples of different geometry (wafers, wedge bars, convex lens), with thicknesses between 0.1 and 8 mm and with different surface treatments (cleaved, lapped, polished, coated with passivating layers) were used in the present study. To monitor the variation of bulk carrier lifetime with the dopant concentration, n- and p-type Ge material with resistivities between 0.01 and 40 Ω cm was studied. Table I gives an overview of the various silicon and germanium materials that were investigated in this work.

Characterization techniques.— The transients of the excess carrier decay in the Si samples were investigated by microwave probing for low and moderate excitation levels and by infrared absorption of free carriers[4-7] for high injection levels.

The infrared absorption by free carriers technique[6,7] is based on the probing of the pulsed excited sample area by IR (1.15, 1.5, or 3 μm wavelength) continuous-wave (CW) beam of either a He-Ne laser or a light-emitting diode (LED). In the case of IR laser probe,

Table I. Si and Ge samples investigated in this study.

Si	S-I			S-II	
Type	FZ and CZ p -type Si			MCZ p-type Si	
Resistivity (Ω cm)	FZ: 1000,100; CZ: 12, 5, 1, 0.5, 0.15 and 0.03			7000	
Geometry	Wafers between 0.28 and 5 mm thick			Wafer pieces 20 × 20 mm^2, 0.28 mm thick	
Ge	**G-I**	**G-II**	**G-III**	**G-IV**	**G-V**
Type	CZ p- and n-type	CZ p-type	FZ p-type	CZ p-type	Optical-grade
Resistivity (Ω cm)	p: 28, 22 and 0.01 n: 37, 21 and 0.15	35, 19, 0.4, 0.1 and 0.07	40	3, 5, 9 and 17	
Geometry	Wafers	As-cut wafers and wedge	Wedge	Bar	Plain-parallel filter and convex lens
Thickness (mm)	0.175 and 0.55	2-4 and wedge	0.1-8	3 × 5 × 20	3.0
Surface preparation	Polished and passivated	Lapped and polished	Cleaved and polished	Lapped	Anti-refl. coat.
Structure	Substrate	Substrate		Electrodes supported (3)	Ge IR filter and AGA lens

the sample is oriented at Brewster angle relatively to an IR probing beam to avoid multireflection effects. Using an LED is preferred due to its low coherence length when its intensity is large enough to obtain a measurable photoresponse. The IR absorption technique can be used with success at excitation densities of the excess carriers larger than 10^{15} cm^{-3}, due to the photon absorption cross section that is smaller than 10^{-18} cm^2. The threshold excitation densities to have a measurable IR photoresponse also depend on the sample thickness, on the resistivity of the material, on the probing beam wavelength, etc. The small influence of carrier trapping effects within the carrier decay transients is an advantage of the IR probing technique.

The absorption by free carriers increases with wavelength and becomes nearly invariable for the frequency range of microwaves (MW). The absorption coefficient at MW exceeds that for IR light. Therefore, the MW absorption technique is most suitable to record transients at low and moderate injection levels. The photoresponse might indeed become nonlinear with respect to amplitude variations due to large absorption coefficient for high densities of excess carriers. Therefore, a comparison of carrier decay parameters measured by MW and IR techniques in the same sample can be obtained for moderate excitation densities. The good agreement between these parameters, measured by the MW and IR techniques at the same excitation density, has been confirmed in Si samples of different resistivities. The transients of the excess carrier decay in the Ge samples were examined by combining MW reflection (MWR) and absorption (MWA) probing of the sample after pulsed excitation.[3,6,7] The MW probing was carried out by using a slit antenna with a 120 μm wide slit for MWR (at 21 GHz) and a 500 μm wide slit for MWA (at 10 GHz). A needle-tip antenna was used for MWR when high spatial resolution was needed. Excess carriers were generated by YAG lasers using 1062 and 1064 nm wavelengths and pulses of 700 ps or 10 ns. The MWR and contact photoconductivity (CPC) transients were measured simultaneously in samples with deposited electrodes. In the germanium wafers, the variation of the excess carrier decay was examined by MWR and MWA as a function of the excitation level and wavelength.[3,7]

Observations.— The measurement techniques and the sample preparation that were used allow us to differentiate between surface recombination, trapping, and recombination effects as discussed in the following paragraphs.

Surface recombination characteristics.— The influence of surface recombination is difficult to avoid even in passivated samples, as illustrated in Fig. 1 and 2 for silicon and germanium samples, respectively. An initial fast decay component can be observed in the excess carrier density variation. This initial fast decay can be attributed to a transitional process caused by surface recombination.

In Si, the separation of the influence of the surface recombination is difficult when using a nearly homogeneous excitation throughout the bulk of the material, as is obtained with 1064 nm pulsed light. In this case the dynamic range of variation of the amplitude of the main decay mode is narrow (curve 1 in Fig. 1). Thereby, a significant decrease of this amplitude can be highlighted by exploiting a sharp excitation profile with initial depth of about 1 μm that can be obtained by using a shorter excitation wavelength of, e.g., 532 nm. The surface and bulk recombination processes compete at low or moderate excitation densities when using an MW probe, as illustrated in Fig. 1 (top). At high excitation densities, defect-associated recombination processes compete with nonlinear carrier decay channels. A typical decay transient measured using an IR CW probe is illustrated in Fig. 1 (bottom). When nonlinear recombination processes are involved, the recombination parameters can be extracted only by simulation and fitting of the whole decay transients by assuming a set of recombination parameters, as indicated in Fig. 1 (bottom).

The absorption coefficient of 1.5×10^4 cm^{-1} (Ref. 8) for Ge leads to the generation of an excess carrier concentration that is strongly depth dependent. Furthermore, as illustrated in Fig. 2, a significant decrease of the amplitude of the main decay mode[3] can clearly be observed when comparing the same sample after passivation (curve 1) and after removing the passivating layer by etching (curve 2). In addition, even the asymptotic lifetime differs in the passivated and the etched samples due to the significant change of the surface recombination velocity s.

The effective lifetime variation as a function of the sample thickness can be used for the estimation of surface recombination as illustrated in Fig. 3 for Si, and in Fig. 4 for n- and p-type Ge both for passivated and lapped samples. The effective lifetime τ_{eff} of the main decay mode can be roughly approximated by $\tau_{\text{eff}} = [1/\tau_b + 1/(\tau_s + \tau_D)]^{-1}$ as the result of both a bulk (τ_b) and a surface component. The surface component results from a component τ_D related to carrier diffusion with $\tau_D = d_{\text{eff}}^2/\pi^2 D$ and a component τ_s related to surface recombination s with $\tau_s = d_{\text{eff}}/s$. Here, d_{eff} is the effective sample thickness, while D is he carrier diffusion coefficient. As illustrated in Fig. 3, a saturation of the effective lifetime is observed in Si for the thickest sample in which case the surface recombination becomes limited by carrier diffusion. For passivated pure Ge material, the surface component dominates or $\tau_s < \tau_D, \tau_b$. The lower the s value is, the steeper the $\tau_{\text{eff}} = f(d_{\text{eff}})$ dependence is, as can be observed in Fig. 4. For bare surfaces and moderately doped material, carrier recombination is dominated by bulk recom-

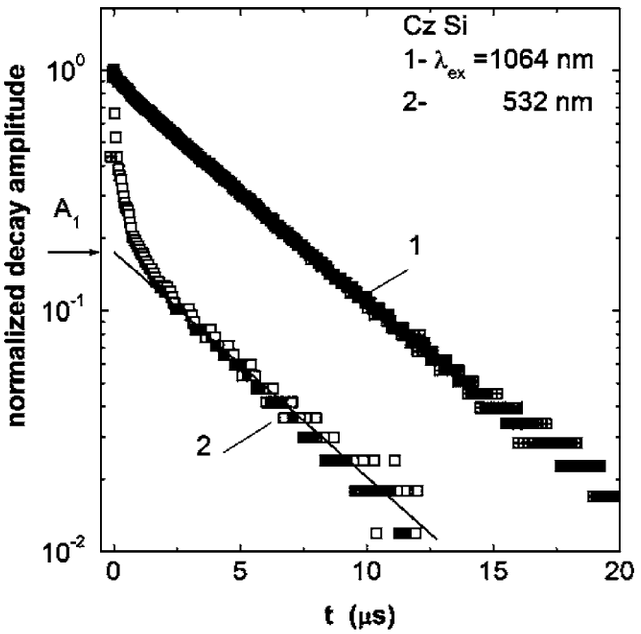

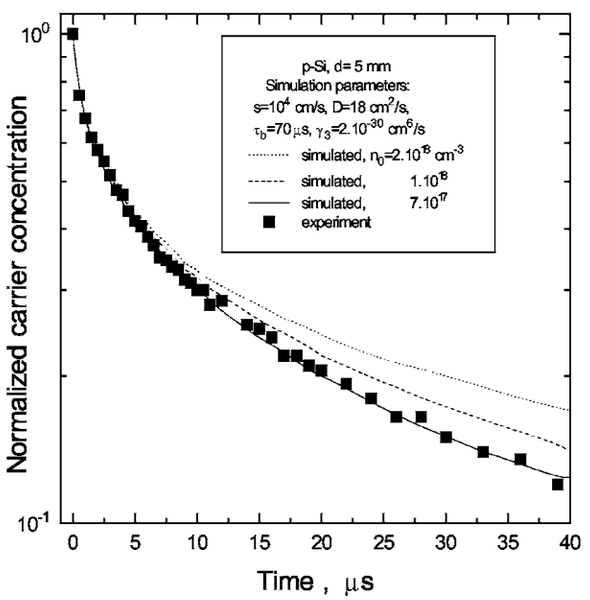

Figure 1. Top: Carrier decay transients in an n-Si sample at different excitation wavelengths at low excitation level measured by MW probe technique. Bottom: The carrier decay transient in p-Si measured at high excitation level (wavelength 1064 nm) by the IR light probe technique is compared with simulated transients calculated by varying the excess carrier density from 7×10^{17} to 2×10^{18} cm^{-3} assuming a bulk lifetime $\tau_b = 70$ μs, a surface recombination velocity $s = 10^4$ cm/s, an ambipolar carrier diffusion coefficient $D = 18$ cm/s, and an effective Auger coefficient $C_p = 2 \times 10^{-30}$ cm^6/s.

bination and fast surface recombination. Therefore, the τ_{eff} values are significantly lower than for passivated pure material, and the slope ($\sim 1/s$) of the τ_{eff} dependence on d_{eff} is smaller.

In Si, s is of the order of 100 and 4×10^3 cm/s, for passivated and polished samples, respectively. The surface recombination velocity s for bare Ge surfaces is estimated to be larger than 10^3 cm/s. The value of s increases with decreasing surface finishing quality as is evident when comparing passivated (p) with lapped (l), freshly

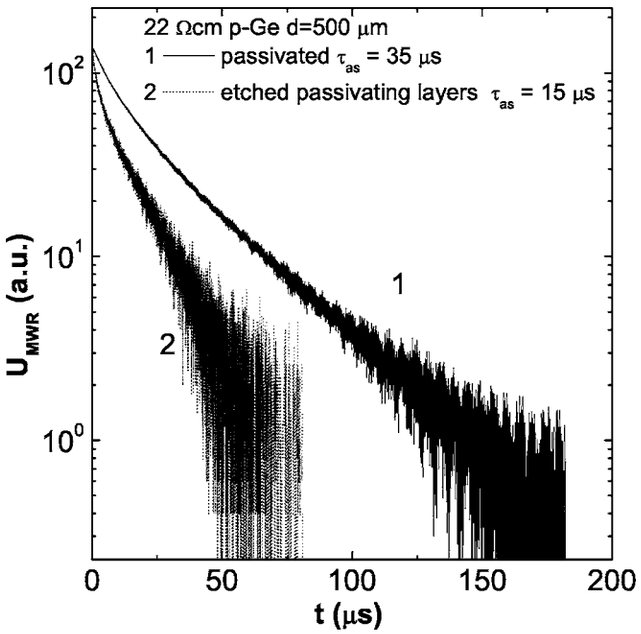

Figure 2. Carrier decay transients in a Ge sample both as-etched and with a passivated surface.

cleaved (c), and polished (p) surfaces of the same Ge substrate yielding $s_p < s_c < s_p < s_l$. Surface recombination has a clear influence on the carrier decay lifetime up to moderately doped material.

A more precise procedure for the separation of surface and bulk recombination parameters is based on measurements at different experimental conditions to have a complete system of independent equations, combined with simulation iterations. The precision of the separation depends on the ratio of the lifetimes ascribed to surface and bulk recombination as well as of the carrier diffusion param-

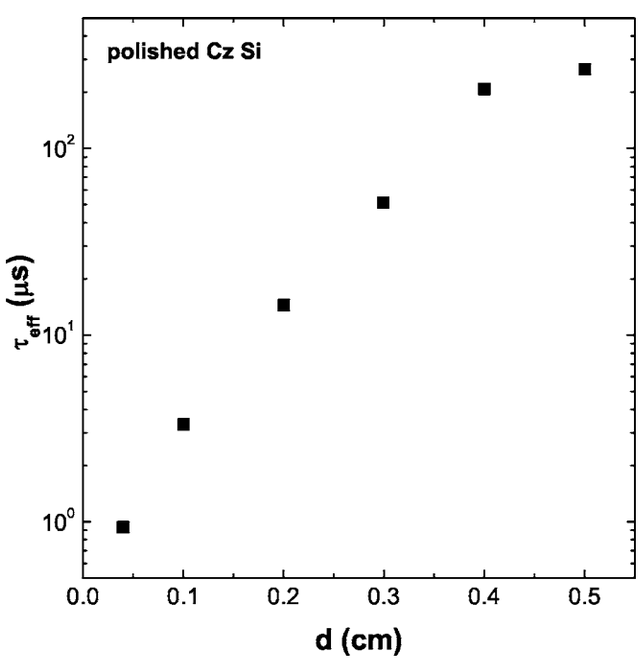

Figure 3. Effective carrier lifetime dependence on sample thickness in polished CZ Si samples measured at low excitation level.

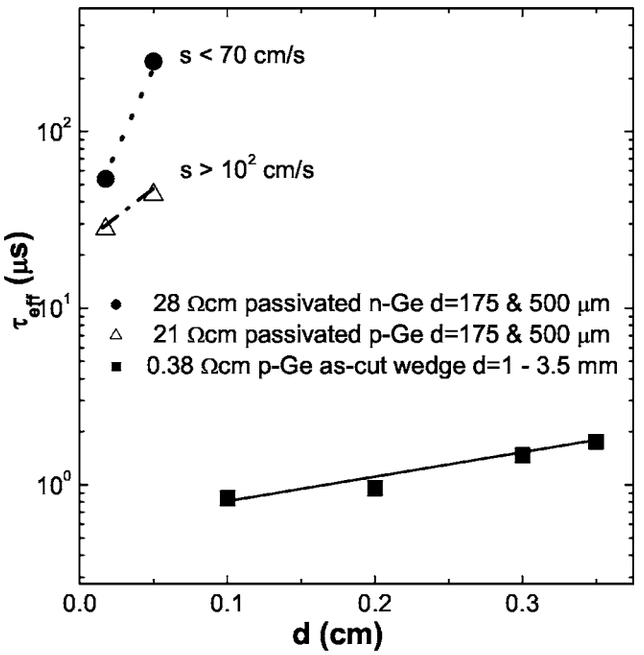

Figure 4. Effective lifetime dependence on sample thickness in n- and p-Ge samples with different doping and surface state.

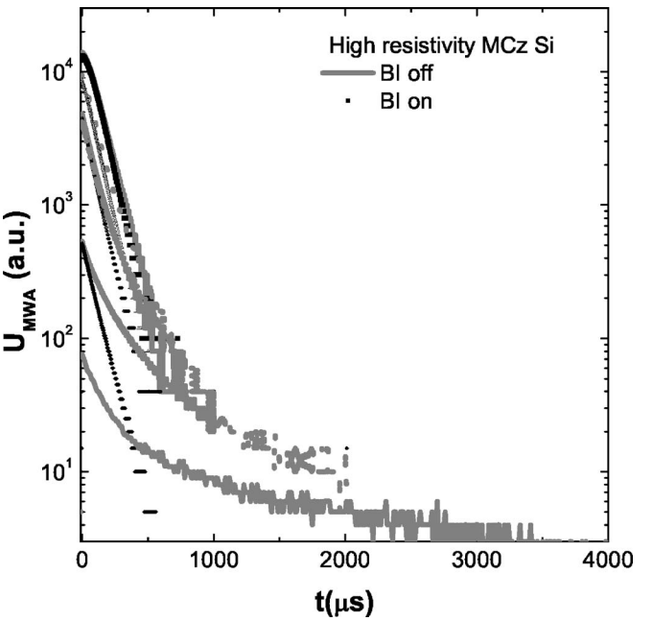

Figure 5. Manifestation of trapping in high-resistivity Si revealed in the excess carrier decays for different excitation levels (proportional to the initial amplitude), with and without bias continuous wave IR illumination (BI).

eters, and also on the experimental errors. Errors in determination of the parameters increase and the separation of parameters becomes difficult, when, e.g., the bulk lifetime is very high and the surface passivation does not allow τ_s to increase sufficiently. The use of thick samples is a possible solution to determine the absolute values of long bulk lifetimes. In the case of asymmetric surface recombination and of high bulk lifetimes, additional measurements are needed, such as cross-sectional scans of decay transients in thick samples to reach a diffusion limited recombination regime[6] whereby bulk recombination dominates within sample depths exceeding the diffusion length. The experimental errors must be lower than 5% if a set of s, τ_b, and D is to be determined simultaneously.[5] In these cases, fitting of the whole decay transients[5] by exploiting the one-dimensional continuity equation model[3,9,10] can successfully be used, allowing these transients to be reproduced at several excitation profiles (wavelengths). Certainly, these simulations are time-consuming but allow a high precision of absolute values to be obtained.

Trapping characteristics.— Significant trapping requires the existence of a system of at least two competing levels, one of which is the dominant recombination center and acts on the carriers of both bands, while the other one acts as trapping center and redistributes carrier flows of only one band. The effect of recombination combined with trapping can be described by the instantaneous decay lifetime τ_{in}[11]

$$\tau_{in}[t(n_{ex})] = \tau_R\left(1 + \frac{N_{tr}N_{Ctr}}{(N_{Ctr} + n_0 + n_{ex})^2}\right) \qquad [1]$$

whereby the recombination lifetime τ_R is increased due to trapping. It is assumed that the observed hyperbolic-like decay at low excitation level is due to trapping by traps in the bandgap with a concentration N_{tr}. It is also assumed that the final states available for thermal release of carriers in recombination-trapping statistics are reduced by thermal activation of the traps leading to a reduced effective density of states $N_{C,Vtr}$, given by $N_{C,Vtr} = N_{C,V}\exp[-|E_{C,V} - E_{tr}|/kT]$ in the conduction (N_C) or valence (N_V) band, respectively.[11] $N_{C,Vtr}$ depends on energy depth $|E_{C,V} - E_{tr}|$ of the trap level E_{tr} for thermal emission at temperature T, k is the Boltzmann constant, while n_0 denotes the equilibrium carrier concentration and n_{ex} is the light-induced excess carrier density. In order to separate the pure recombination revealed by τ_R, the capture into a trapping level can be suppressed by saturating the traps either by increasing n_{ex}, thus making the term $N_{tr}N_{CM}/n_{ex}^2$ much smaller than 1, or by using IR-rich bias illumination to quench the trapping-induced photoconductivity. The character of the decays is however somewhat different for both of these methods to suppress trapping, as is illustrated for Si in Fig. 5. In the case of Si, the trapping-related long tail is very sensitive to the level, $\sim n_{ex}$, of bulk excitation. Due to this it is difficult to examine recombination lifetime in high-resistivity material using low excitation levels. In pure Ge material, however, a trapping effect can be observed even when using a sharp excitation profile, as illustrated in Fig. 6. Significant trapping is always revealed by two-component, hyperbolic-like decays, and as such it is very similar to the transients caused by surface recombination and Auger processes. A separation of both processes is only possible by careful experiments, varying the relevant experimental parameters.

In germanium, the effective (asymptotic) lifetime significantly varies with excitation level, material type, and resistivity, as is illustrated in Fig. 7 and 8. In pure material, τ_{eff} slightly decreases when applying additional broadband steady-state illumination at the lowest excitation levels. In moderately doped material, τ_{eff} increases with the excitation level, when some threshold excitation level is reached. This increase can be explained by filling of the recombination centers,[12] when the excess carrier concentration approaches the number of recombination centers. Such behavior implies that the SRH assumption of carrier pair recombination lifetime is no longer valid. Due to this the carrier transient again becomes complex with an asymptotic decay determined by the longest of the effective time constants. In 3 Ω cm p-Ge, for instance, effective trap filling occurs for an average excess carrier density above 10^{16} cm^{-3}. The surface traps are most probably saturated by the excess carriers, which is a well-known surface effect in Si.[13,14] The carrier profile is smoothened toward the bulk by carrier diffusion, however, with a significantly decreased density. In heavily doped material, bulk recombination dominates and the carrier decay transients consist only of one component as can be seen in Fig. 8. To obtain a sufficient photore-

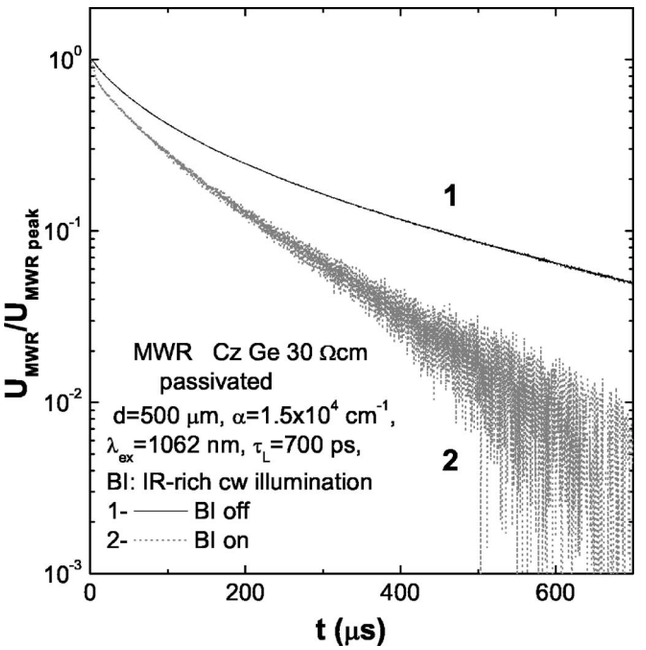

Figure 6. Similar trapping effects in Ge with and without the use of background bias illumination.

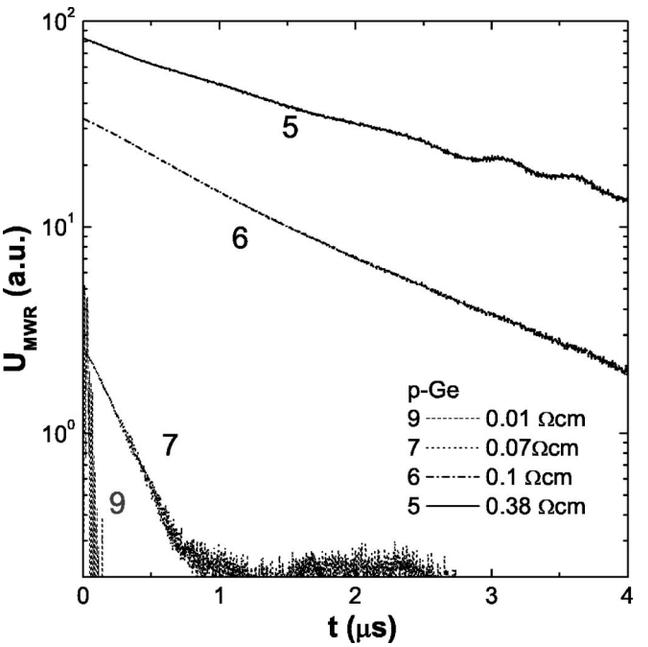

Figure 8. MWR transients in heavily doped Ge samples.

sponse in the high-conductivity material, the excess carrier density has to be increased proportionally to the doping level. The effective lifetime is also to a significant extent determined by bulk recombination. The latter depends on the crystal fabrication technology and on the crystal resistivity. Decay transients measured in different materials are illustrated in Fig. 7 and 8. The longest decays in the range of 2 ms are obtained in the FZ high-resistivity sample after fresh cleaving. A long asymptotic lifetime is measured also in optical-grade Ge, although in the latter material a clear two-component decay is inherent, which can be related to trapping and trap filling. It is known that this material contains grain boundaries which might be the reason for the observed trapping and trap filling.

Decay transients which correspond to carrier lifetimes of hundreds of μs in low doped CZ Ge are reduced to the nanosecond scale (Fig. 8) when the resistivity decreases from 35 to 0.01 Ω cm. Taking into account the impact of the surface, the bulk lifetime τ_b is estimated to be of the order of 500 μs in the 40 Ω cm p-type FZ sample, of 260 μs in the 20–30 Ω cm high-purity n- and p-type CZ material, while it is only 30 ns in 0.01 Ω cm p-Ge.

In CZ grown Si samples, the carrier recombination lifetime, measured at high excitation level, is nearly invariant up to heavily doped material. In FZ and MCZ grown material, the carrier lifetime is significantly higher and the lifetime variation with excitation level is more pronounced.

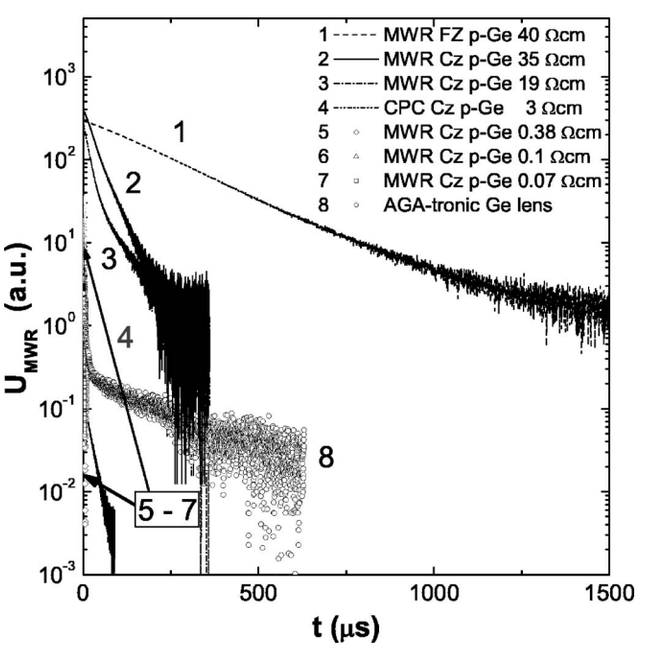

Figure 7. MWR transients measured in Ge samples with various resistivities.

Comparative analyses of carrier lifetime variation with doping and excitation level in Si and Ge.— The present analysis of the lifetime variation with dopant concentration was limited to p-type Si and Ge material, while similar characteristics were observed for n-type material. The variation of recombination lifetime in Si is illustrated in Fig. 9. Open diamond symbols represent the lifetime values measured in p-Si at high excitation level in the present study, while the solid and open circles are published data generalized in Ref. 1. The stars and crosses show carrier lifetimes determined in the present investigation in MCZ p-Si using low excitation. It is clear that the lifetime variation in CZ Si observed at high excitation density in the present experiments correlates well with the one reported in Ref. 1. This group of experimental data and the high injection level data of the present study are described well by the expression

$$\tau = 1/(\tau_R^{-1} + C_p n_{dop}^2) \qquad [2]$$

assuming the simultaneous action of linear recombination, characterized by a recombination lifetime τ_R of 40 μs, and Auger recombination with an Auger coefficient C_p of 10^{-31} cm^6/s as is shown by curve 1. For heavy doping, the Auger process becomes clearly dominant. The upper open circles set of experimental values can be roughly approximated by Eq. 2 using a recombination lifetime τ_R of 800 μs as illustrated by curve 2 in Fig. 9. At low doping the esti-

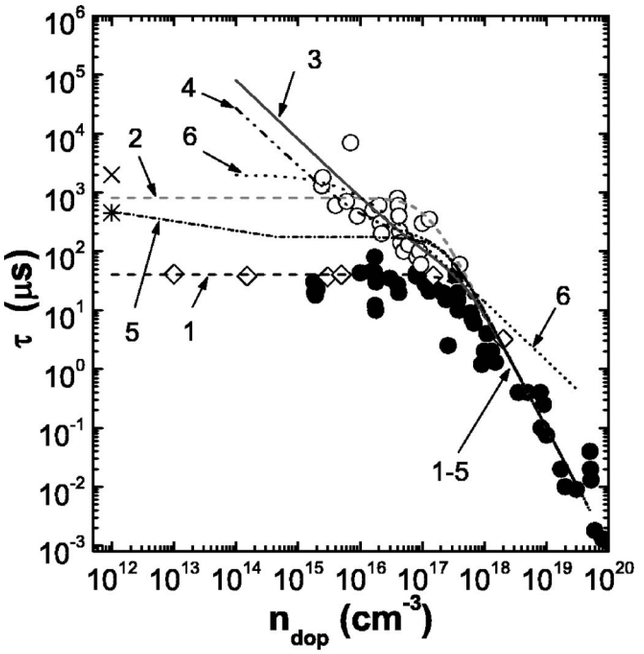

Figure 9. Carrier lifetime variation with doping in Si. The open diamond symbols represent lifetime values measured in p-Si at high excitation level, while stars and crosses show lifetime values determined in the present study in MCZ p-Si at low excitation level. Solid and open circles represent the generalized data of Ref. [1] for p-Si. The solid curves 1 and 2 represent simulated lifetime values assuming the simultaneous action of linear (with constant lifetime τ_R) and Auger recombination processes with an Auger coefficient C_p of 10^{-31} cm^6/s. Curves 3–5 represent simulations with τ_R dependent on injection level according to the SRH theory and with $L = 0.01$ for curve 3, $L = 2$ for curves 4 and 5. The other parameters are $E_R = 0.17$ eV for curves 3 as well as 4 and $E_R = 0.38$ eV for curve 5, while $\tau_{p0} = 200$ μs, $\tau_{n0} = 40$ μs. Curve 6 represents an approximation using Eq. 3 with constant $\tau_{SRH} = 2$ ms and $n_{thr} = 7 \times 10^{15}$ cm^{-3}.

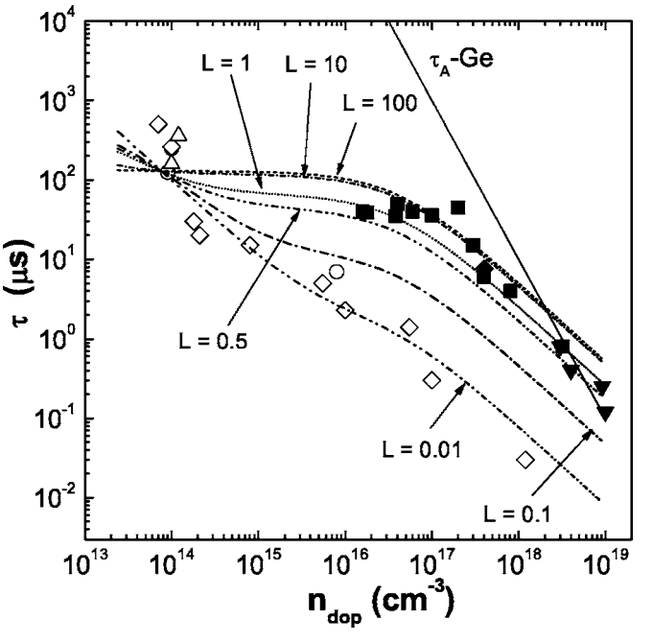

Figure 10. Variation of carrier recombination lifetime as a function of dopant concentration estimated from the Ge material resistivity. The open symbols represent the lifetime values measured in this work while the closed symbols show published data from Ref. 13 and 14. The line τ_A-Ge is the calculated Auger recombination lifetime using the Auger coefficient of 10^{-31} cm^6/s published in Ref. 13. The curves for L between 0.01 and 100 illustrate the lifetime variations assuming a fixed excitation level $L = n_{ex}/n_{dop}$ for each curve. The curves for different L values are simulated using the SRH model and Eq. 3 with a threshold doping density n_{thr} of 4×10^{16} cm^{-3} in p-Ge. The other parameters used are $E_R = 0.3$ eV, $N_R\sigma_p = 10^{-3}$ cm^{-1}, $N_R\sigma_n = 10^{-1}$ cm^{-1}. The variation of the SRH lifetime was calculated according to the well-known expressions given in Ref. 1 and taking into account the excitation level $L \sim n_{ex}$.

mate from Eq. 2 obtained by extrapolating the simulated lifetime variation associated with the open circles set is close to the lifetime value measured for MCZ p-Si in the present study. The carrier lifetime variation with doping for Si is thus in good agreement with Eq. 2, which is based on SRH and Auger recombination theory. τ_{SRH}, however, has to be adjusted to the carrier injection level and to the material quality which is characterized by different prevailing recombination centers and the experimental conditions.

The lifetime variation for the open circle set data differs however in details from that approximated by Eq. 2, keeping a constant τ_R. A better fit can be achieved by replacing the constant τ_R with an excitation level-dependent τ_{SRH} with varied E_R and L, as illustrated by curves 3–5 in Fig. 9. The fitting parameters are chosen as $L = n_{ex}/p_0 = 0.01$ for curve 3, $L = 2$ for curves 4 and 5 in Fig. 9. The other parameters are $E_R = 0.17$ eV for curves 3 as well as 4 and $E_R = 0.38$ eV for curve 5, while $\tau_{p0} = 1/\upsilon\sigma_p N_R = 200$ μs, $\tau_{n0} = 1/\upsilon\sigma_n N_R = 40$ μs, with respective values of thermal velocity υ, capture cross section $\sigma_{n,p}$, activation energy E_R, and concentration N_R of recombination centers. In Si material with relatively large τ_R, traps (trapping centers in the case of high-resistivity material) and doping-induced recombination defects (for moderately doped material) play an important role. In heavily doped Si material, the Auger process clearly dominates. However, for the open circle set, the lifetime variation can roughly be approximated by a $1/n_{dop}$ dependence and in general by the empirical approximation

$$\tau_R = \tau_{SRH}(1 + n_{dop}/n_{thr}) \qquad [3]$$

assuming a threshold doping density n_{thr}, as suggested in Ref. 2, starting from which the generation of traps associated with the dopant seems to become important. Thereby, the open circles set taken from Ref. 1 also can be described rather well by Eq. 3 for $p_0 = n_{dop} < 10^{18}$ cm^{-3} and using $n_{thr} = 7 \times 10^{15}$ cm^{-3}.[2] This is illustrated by the dotted line 6 in Fig. 9. The nature of these dopant-related traps is unclear at this moment. As discussed further, a similar behavior is however also observed for germanium. Equation 3 should be considered as phenomenological and the simplest (first-order) approximation of lifetime variation over a wide range of dopant concentrations which contains only one parameter (n_{thr}) instead of a set of not well-defined parameters connected with Auger interband recombination, Auger trap assisted recombination, presence of dopant related traps, etc.

The variation of recombination lifetime τ_R with dopant concentration n_{dop} measured in this work in p-Ge at low excitation level, is shown in Fig. 10 by the open symbols. These τ_R values are compared with those determined in Ref. 15 and 16, which are represented by the closed symbols in the same figure. The variation of the recombination lifetime measured in Ge agrees well up to $n_{dop} \sim 10^{16}$ cm^{-3} with τ_{SRH} for low injection level. A fixed recombination center concentration can be assumed for a doping concentration below 10^{16} cm^{-3}. The observed further decrease of lifetime for $n_{dop} > 10^{16}$ cm^{-3} is again described well by Eq. 3 and can be attributed to an increase of recombination center concentration proportional to the dopant concentration. The lines ($L = 0.01$–100) in Fig. 10 represent the recombination lifetimes as a function of dopant concentration, simulated using Eq. 3 and τ_{SRH} calculated by well-known expressions[1,12]for different excitation levels defined by $L = n_{ex}/n_{dop} \equiv n_{ex}/p_0$ in the p-type material, i.e.

$$\tau_{SRH} = \frac{\tau_{n0}(p_0 + N_V e^{-(E_R - E_V)/kT} + n_{ex}) + \tau_{p0}(n_0 + N_C e^{-(E_C - E_R)/kT} + n_{ex})}{n_0 + p_0 + n_{ex}} \quad [4]$$

Assuming $n_{thr} = 4 \times 10^{16}$ cm^{-3} in Eq. 3 and calculating τ_{SRH} by using Eq. 4, the simulated recombination lifetime decrease is in good agreement with the experimental results obtained at low excitation level. This threshold value n_{thr} is also in agreement with $n_{ex} \sim 10^{16}$ cm^{-3} estimated in 3 Ω cm Ge from the trap filling effect[12] dependence on excitation level. A similar lifetime dependence on doping is thus observed in Si and Ge and can be well approximated by Eq. 3.

The simulated curves for L varying between 0.01 and 100 show the expected lifetime dependence on excitation level and doping, assuming a linear increase of excess carrier density $n_{ex} = Ln_{dop}$ with doping, i.e., keeping the excitation level L invariant along the same curve while n_{dop} is varying. The excitation density in the present study is varied via absorption of pulsed IR light. The curves for $L = 0.01$ to 100 were simulated using Eq. 3 with the same threshold doping density n_{thr} of 4×10^{16} cm^{-3} while varying L and using a fixed value for the product $N_R\sigma_{p,n}$ of trap concentration N_R and trap capture cross section $\sigma_{p,n}$ for holes (p) and electrons (n), respectively. The lifetime values, simulated as a function of excitation level $\sim n_{ex}$, show an increase with excitation level (fixed by L). The simulated curve 4 at $L = 1$ agrees well with the experimental data of Ref. 15 and 16. Thus, our experimental data are in agreement with those of Ref. 15 and 16 using the same trap parameters, i.e., $N_R\sigma_p = 10^{-3}$ cm^{-1} and $N_R\sigma_n = 10^{-1}$ cm^{-1}, when differences in excitation level are taken into account. Moreover, the curves ($L = 0.5$–100) that are simulated for high excitation levels L in the range from 0.5 to 100 cover most of the experimental values published in Ref. 15 and 16. This implies that the data in Ref. 15 and 16 were obtained at elevated injection levels to induce an observable photoconductivity signal. An increase of the lifetime values with excitation level was also observed in our experiments and is due to the trap filling effect, which can be observed when using short excitation pulses and which cannot be observed in experiments with long excitation pulses, as probably applied in Ref. 15.

The agreement obtained for p-Ge over a wide range of dopant concentrations n_{dop} is quite good, taking into account the uncertainty on the n_{ex}/n_{dop} estimation. The deviations between the experimental values for n-Ge, for optical-grade Ge and high purity FZ p-Ge and those simulated for p-Ge ones are however noticeable. This is probably related to a defect with different capture cross section and density that is controlling the carrier lifetime. This is also corroborated by the different character of the carrier decays obtained for optical-grade Ge material in our experiments. Also for Ge, for doping densities above n_{thr}, the simple SRH model is insufficient, and this is taken into account by the term $(1 + n_{dop}/n_{thr})^{-1}$ in Eq. 3. The nonlinear Auger recombination, shown schematically by the τ_A-Ge line in Fig. 10, seems to be negligible in the investigated n_{dop} range if the Auger coefficient is much smaller than 10^{-30} cm^6/s. Analysis of the correlative effects[17] does not improve the fit of the lifetime decrease sufficiently when taking into account Auger processes in heavily doped Ge. Moreover, the role of excess carriers also should be included at increased n_{ex} when evaluating the Auger coefficient values. In the case of a sharp excitation profile, surface defects can also be the reason for the variation of the absolute τ values and the deviation from the expected bulk lifetime dependence on doping.

In Ge, the impact of the Auger process in heavily doped material seems not to be as strong as in Si. The more extreme lifetime measurement conditions could be a reason, as Auger recombination is a nonlinear process at the elevated excitation levels that are needed to obtain a measurable photoresponse on top of the background of the equilibrium free carrier absorption. The sharp excitation profiles exploited in the experiments with Ge also complicate significantly the lifetime measurement procedure. In that case the domain of excited carriers indeed becomes a system of distributed parameters with nonlinear recombination and inhomogeneous injection. Contrary to Ge, the experiments with Si can however be performed with a nearly homogeneous excitation level by using laser sources, even in heavily doped material.

An advanced theory of the extraction and separation of recombination parameters of several levels recently has been proposed.[18,19] A clever idea for obtaining additional information is based on the increase of the excitation density to force the decay process into a nonlinear regime when higher recombination harmonics dominates the initial fast recombination decay. However, this simulation and measurement technique will only yield useful results, when Auger type and surface recombination processes can be ignored, i.e., in the range of low and moderate doping and injection levels and for well passivated samples. A very high precision of the experimental data is necessary to solve the large number of characteristic equations obtained including higher recombination lifetime modes with experimental parameters. Significant computational resources are needed to solve (for more intricate experimental regimes it becomes even impossible) this large set of characteristic equations. This approach can be fruitful in practice when a precise separation of several trap levels is performed at very well-defined and implemented measurement conditions. However, this advanced lifetime spectroscopy method is difficult to apply in practice over a wide range of doping and excitation levels.

Conclusions.— The carrier lifetime variation with doping in p-Si can be modeled well by assuming the simultaneous action of linear and Auger recombination processes with an Auger coefficient C_p of 10^{-31} cm^6/s and a carrier lifetime τ_{SRH} dependent on carrier trap properties and on the carrier injection level. In Si material with relatively large τ_R, additional trapping centers are observed in high-resistivity material while doping-induced recombination defects are observed in moderately doped materials. In heavily doped material with resistivities below 0.2 Ω cm, the Auger process clearly dominates in p-Si.

A similar dependence of carrier lifetime on doping and excitation level was observed in Ge, although for heavily doped Ge the impact of the Auger process is not so strong as in heavily doped Si for similar dopant concentrations. The more complicated lifetime measurement conditions could be a reason for this, as Auger recombination is a nonlinear process at the elevated excitation levels that are needed to obtain a measurable photoconductivity signal. The steep excitation profiles in Ge further complicate the lifetime measurement procedure, whereby the domain of excited carriers becomes a system of distributed parameters with nonlinear recombination and inhomogeneous injection.

The variation of τ_R with doping was clarified for low and elevated excitation levels by a comparison of the observations in Ge of the present study with a wide range of published ones, and could be simulated well by using a constant value of 10^{-1} cm^{-1} for the product $N_R\sigma_n$ of trap density and capture cross section. It was shown that the observations could be explained by the SRH model in low and moderately doped material, whereby the lifetime decreases linearly with $1/n_{dop}$ for dopant concentrations n_{thr} above 4×10^{16} cm^{-3}. This behavior can be attributed to an increase of the recombination center concentration proportional to the dopant concentration.

Acknowledgments

UMICORE, L. Subacius, and V. Grivickas are acknowledged for providing the Ge samples, and J. Harkonen for providing the MCZ Si, that were studied in this work. This work was partially supported by the Lithuanian State Science and Studies Foundation and by the Institute for the Promotion of Innovation by Science and Technology in Flanders (IWT-Vlaanderen).

References

1. D. K. Schroder, *Semiconductor Material and Device Characterization*, Chap. 8, p. 364, Wiley Interscience, New York (1990).
2. J. G. Fossum and D. S. Lee, *Solid-State Electron.*, **2**, 741 (1982).

3. E. Gaubas and J. Vanhellemont, *J. Appl. Phys.*, **80**, 6293 (1996).
4. E. Gaubas and A. Kaniava, *Rev. Sci. Instrum.*, **67**, 2339 (1996).
5. E. Gaubas, A. Kaniava, and J. Vaitkus, *Semicond. Sci. Technol.*, **12**, 1 (1997).
6. E. Gaubas, J. Vaitkus, E. Simoen, C. Claeys, and J. Vanhellemont, *Mater. Sci. Semicond. Process.*, **4**, 125 (2001).
7. E. Gaubas, *Lith. J. Phys.*, **43**, 145 (2003).
8. A. Dargys and J. Kundrotas, *Handbook on Physical Properties of Ge, Si,* GaAs *and* InP, p. 47, 59, SEP, Vilnius (1994).
9. J. P. McKelvey and R. L. Longini, *J. Appl. Phys.*, **25**, 634 (1954).
10. K. L. Luke and L. J. Cheng, *J. Appl. Phys.*, **61**, 2282 (1987).
11. S. M. Ryvkin, *Photoelectric Effects in Semiconductors*, Chap. 6, Consultants Bureau, New York (1964).
12. J. S. Blakemore, *Semiconductor Statistics*, Chap. 8, Pergamon Press, New York (1962).
13. E. Gaubas, J. Vanhellemont, E. Simoen, C. Claeys, P. Clauws, H. Kraner, and G. Vilkelis, in *High purity Silicon IV*, PV 96-13, p. 439, The Electrochemical Society Proceedings Series, Pennington, NJ (1996).
14. S. W. Glunz, D. Biro, S. Rein, and W. Warta, *J. Appl. Phys.*, **86**, 683 (1999).
15. R. Conradt and J. Aengenheister, *Solid State Commun.*, **10**, 321 (1972).
16. D. Poelman, P. Clauws, and B. Depuydt, *Sol. Energy Mater. Sol. Cells*, **76**, 167 (2003).
17. A. Hangleiter, p. 129, Habilitation Thesis, Stuttgart University (1992).
18. D. Debuf, Y. Shrivastava, and A. Dunn, *Phys. Rev. B*, **65**, 245211 (2002).
19. D. Debuf, *J. Appl. Phys.*, **96**, 6454 (2004).